

***Supporting Information for***

***In Situ* Fabricated Cu-Ag Nanoparticle - Embedded Polymer Thin Film  
as an Efficient Broad Spectrum SERS Substrate**

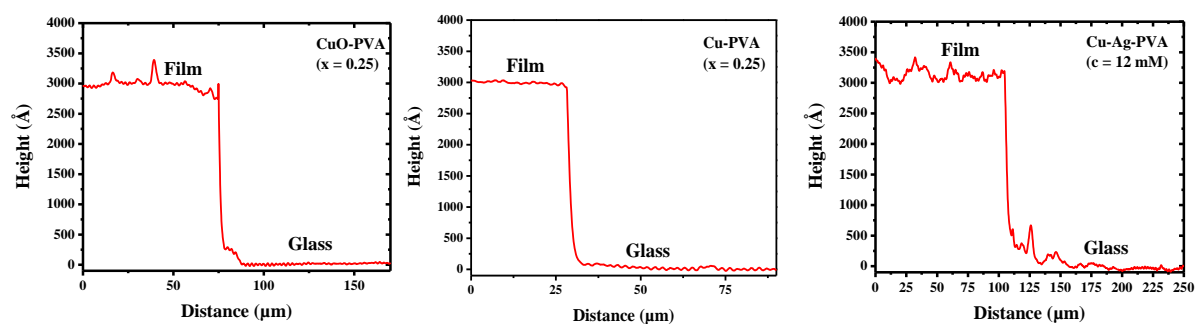
**V. Kesava Rao, Pankaj Ghildiyal and T. P. Radhakrishnan\***  
**School of Chemistry, University of Hyderabad, Hyderabad – 500 046, India**

<b><u>Page</u></b>	<b><u>Contents</u></b>
S2	Thickness of the nanocomposite films (Figure S1)
S3	Estimation of Cu-Ag composition of the bimetal nanoparticles [ICP-OES, EDX (FESEM, TEM)] (Table S1, S2)
S4	Decomposition of $\text{Cu}(\text{NO}_3)_2 \cdot 3\text{H}_2\text{O}$ (Figure S2, S3)
S5	Tauc plots for the CuO-PVA thin film (Figure S4)
S6	AFM images of the CuO-PVA and Cu-PVA thin films (Figure S5, Table S3)
S7	Extinction spectra of the Cu-PVA, Cu-Ag-PVA and Ag-PVA thin films (Figure S6, S7)
S8	TEM images of the Ag-PVA thin films (Figure S8)
S9	Electron diffraction of the CuO, Cu and Cu-Ag-PVA thin films (Table S4, S5)
S10	X-ray photoelectron spectra (Figure S9)
S11-S12	Stability of the Cu-PVA and Cu-Ag-PVA thin films (Figure S10, S11)
S13	Absorption spectra of R6G and MB (Figure S12)
S14	Absorption of analyte on Cu-Ag-PVA Thin Films (Figure S13)
S15-S16	Raman spectra of PVA, Cu-Ag-PVA, Cu-Ag-PVA with R6G, MB (Figure S14, S15, S16)
S17-S19	Calculation of the SERS enhancement factors (Table S6, S7, S8)
S20	Comparison of enhancement factors (Table S9)
S21	Limit of detection

## Thickness of the Nanocomposite Films

Thickness of the different films fabricated as described in the main text was measured using an Ambios Technology XP-1 Profilometer.

**Figure S1.** The line profiles recorded across a sharp edge of the film with respect to the substrate; thickness of the film is found to be  $\sim 300$  nm in all cases.



## Estimation of the Cu-Ag Composition

### ICP analysis of the metal content

Cu-PVA and Cu-Ag-PVA (fabricated using  $\text{AgNO}_3$  solution of concentration, c) and Ag-PVA thin films coated on a  $3 \times 1 \text{ cm}^2$  quartz plate were dissolved in 69% nitric acid. The solution was diluted to 100 ml and ICP-OES analysis was carried out.

**Table S1.** Content of Cu and Ag in the Cu-PVA and Cu-Ag-PVA (fabricated using  $\text{AgNO}_3$  solution of concentration, c) thin films determined using ICP-OES.

Substrate		Atom content in the film ( $\mu\text{mol}$ )		Atom % in the film	
		Cu	Ag	Cu	Ag
Cu-PVA		0.6590	0	100	0
Cu-Ag-PVA [c (mM)]	1	0.6987	0.1954	78	22
	6	0.4572	0.3888	54	46
	9	0.3632	0.4432	45	55
	12	0.2931	0.5431	35	65
Ag/PVA	0.5	0	0.3770	0	100
	1.0	0	0.8292	0	100

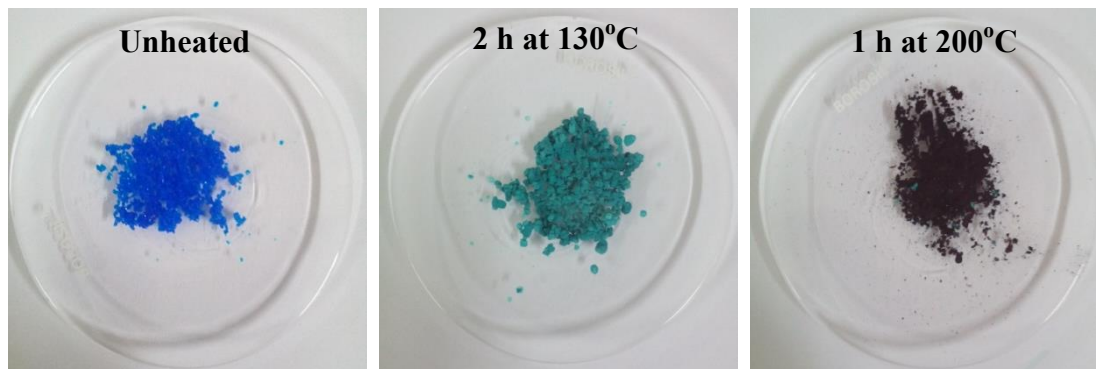
**Table S2.** Cu-Ag compositions of Cu-PVA and Cu-Ag-PVA (fabricated using  $\text{AgNO}_3$  solution of concentration, c) thin films estimated by ICP-OES analysis, compared with that obtained from EDX spectroscopy analysis in TEM and FESEM.

Substrate		Atom%					
		ICP-OES		EDX (TEM)		EDX (FESEM)	
		Cu	Ag	Cu	Ag	Cu	Ag
Cu-PVA		100	0	100	0	100	0
Cu-Ag-PVA [c (mM)]	1	78	22	71	29	70	30
	3	-	-	56	44	62	38
	6	54	46	34	66	45	55
	9	45	55	24	76	28	72
	12	35	65	19	81	24	76

### Decomposition of $\text{Cu}(\text{NO}_3)_2 \cdot 3\text{H}_2\text{O}$

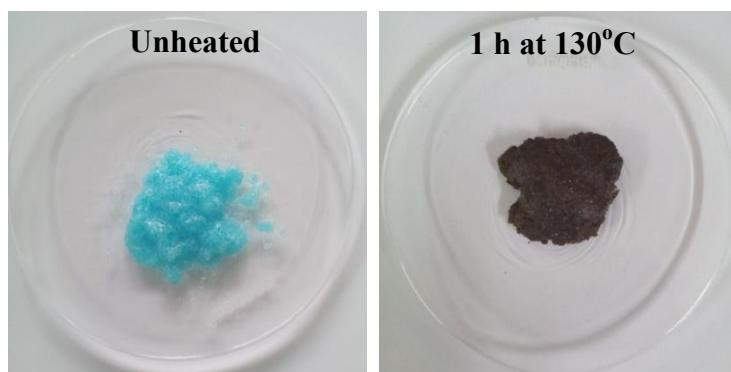
Decomposition of  $\text{Cu}(\text{NO}_3)_2 \cdot 3\text{H}_2\text{O}$  was examined by heating the pure salt as well as its solid mixture with poly(vinyl alcohol) (PVA) at different temperatures.

**Figure S2.** Photographs of  $\text{Cu}(\text{NO}_3)_2 \cdot 3\text{H}_2\text{O}$  heated under different conditions.



Color change observed in the sample heated at 130°C is due to the formation of basic copper nitrate and the black material obtained when heated at 200°C is cupric oxide (confirmed by powder X-ray diffraction experiment and comparison to JCPDS 75-1779 [ $\text{Cu}_2(\text{OH})_3(\text{NO}_3)$ ] and 89-5897 [ $\text{CuO}$ ] respectively). See also: H. W. Richardson, Ullmann's Encyclopedia of Industrial Chemistry, Wiley 2012, p 273.

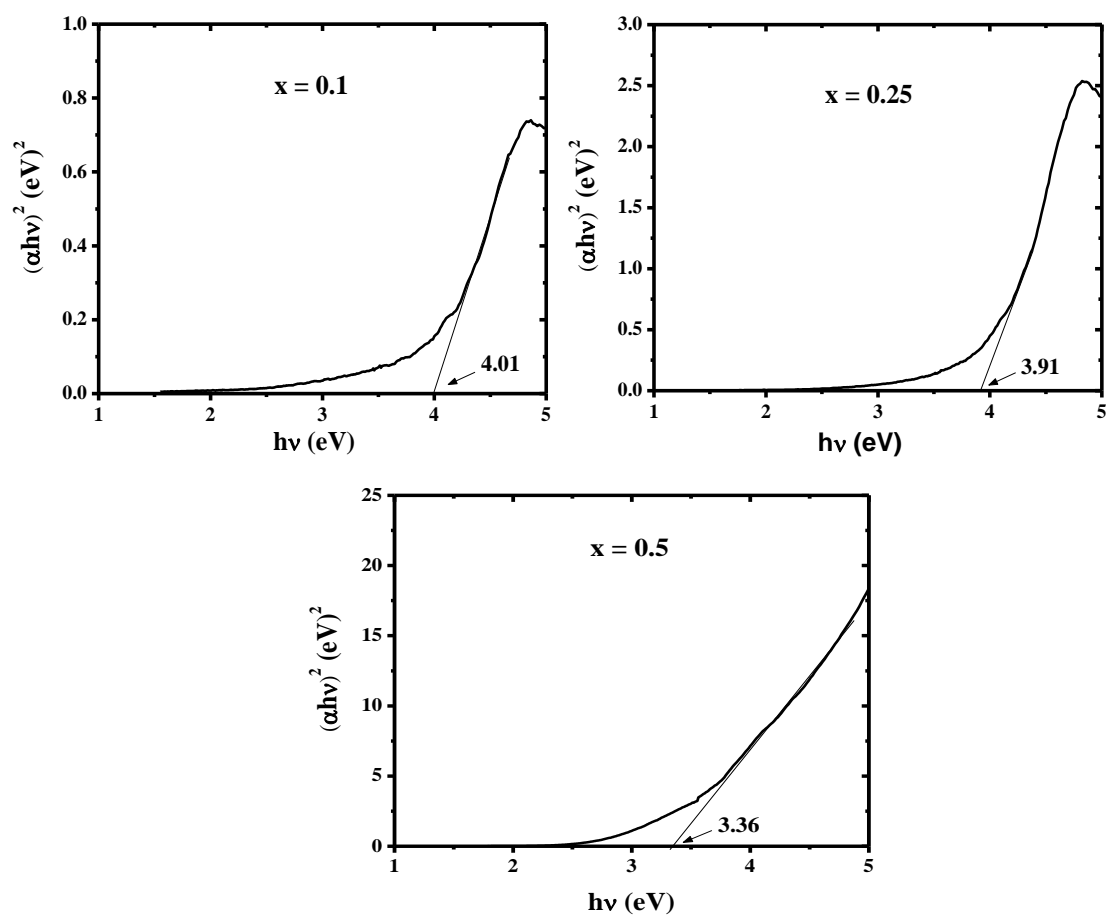
**Figure S3.** Photographs of  $\text{Cu}(\text{NO}_3)_2 \cdot 3\text{H}_2\text{O}$ +PVA heated under different conditions.



Formation of the black solid at 130°C suggests that the presence of PVA lowers the temperature of decomposition of  $\text{Cu}(\text{NO}_3)_2 \cdot 3\text{H}_2\text{O}$  and formation of  $\text{CuO}$ .

### Tauc Plots for the CuO-PVA Thin Film

**Figure S4.** Tauc plots for the direct band gap of the CuO-PVA film with different values of Cu/PVA weight ratio (x).



### AFM Images of the CuO-PVA and Cu-PVA Thin Films

AFM images were taken on CuO-PVA and Cu-PVA thin films to examine the average roughness of the films; an NT-MDT model Solver Pro-M AFM in semi-contact mode with a cantilever having a force constant of 11.8 N/m was used.

The average roughness of both films were found to be  $\leq 0.5$  nm.

**Figure S5.** AFM images and histogram of the surface (height) roughness of CuO-PVA and Cu-PVA thin films.

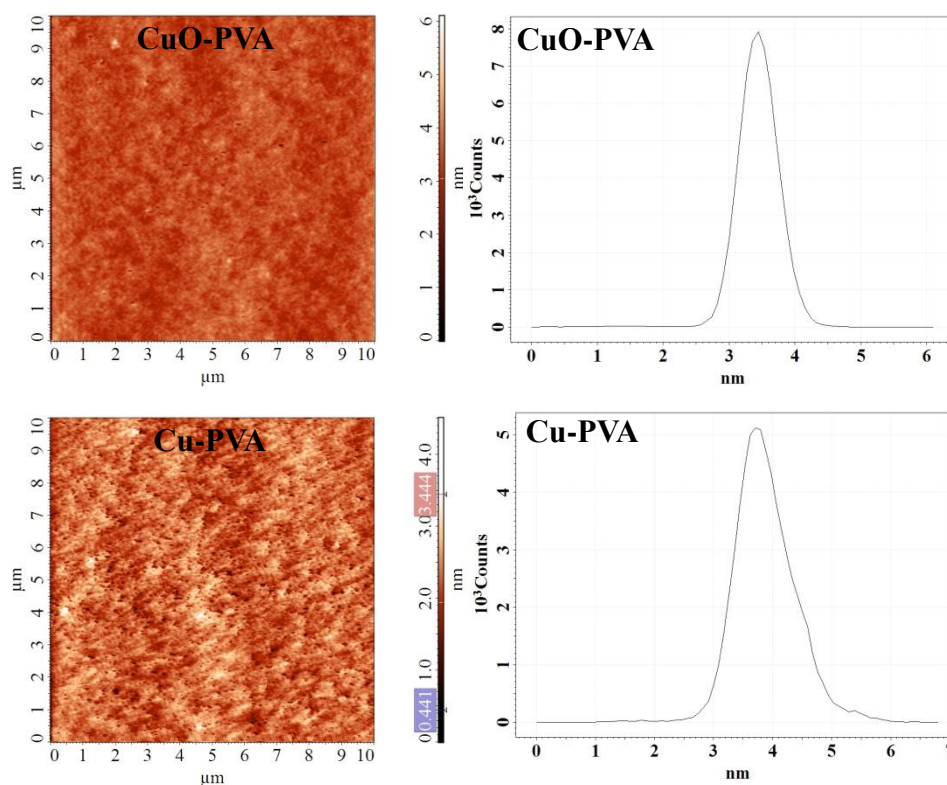


**Table S3.** Average roughness with standard deviation ( $\sigma$ ) inferred from the AFM images taken at 5 different regions ( $10 \times 10 \mu\text{m}^2$ ) on the CuO-PVA and Cu-PVA thin films.

Image	Average roughness (nm)	
	CuO-PVA	Cu-PVA
1	0.63	0.44
2	0.24	0.40
3	0.65	0.41
4	0.26	0.55
5	0.34	0.69
Average for the 5 measurements ( $\sigma$ )	0.42 (0.20)	0.50 (0.12)

### Extinction Spectra of the Cu-PVA, Cu-Ag-PVA and Ag-PVA Thin Films

**Figure S6.** Extinction spectra of the Cu-PVA and Cu-Ag-PVA thin film formed by treatment with different concentrations ( $c$ ) of  $\text{AgNO}_3$  solutions (part of this figure relevant to the main study is provided in Figure 5 of the main text).

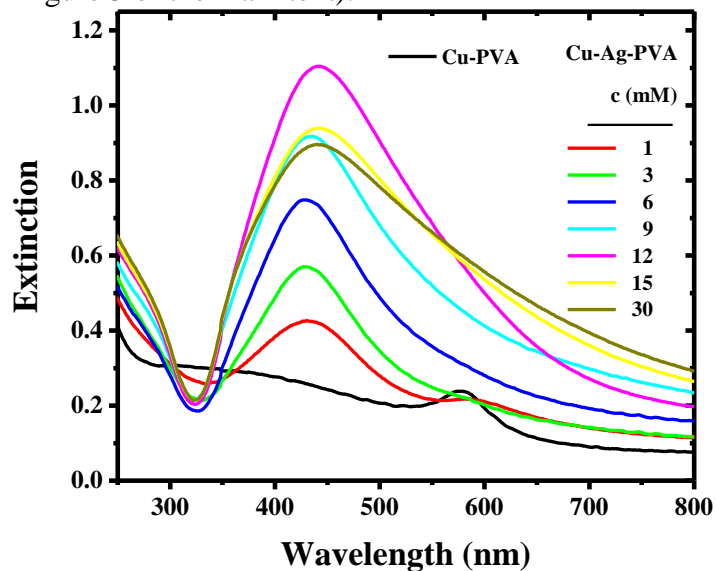
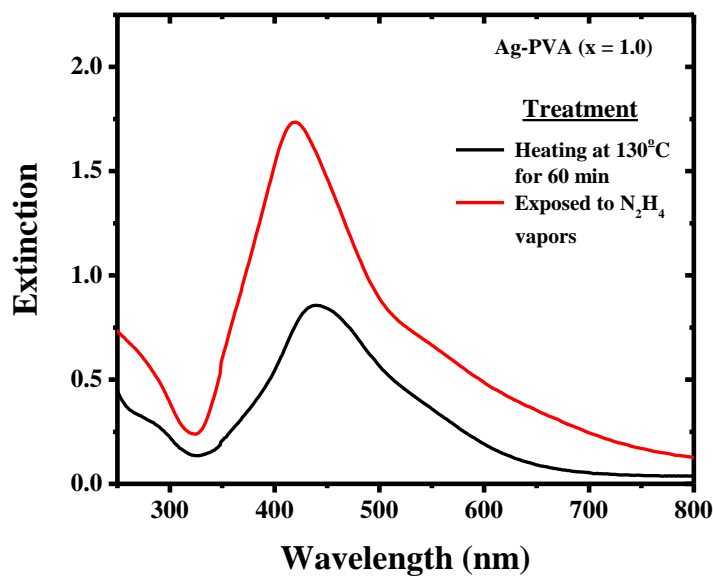
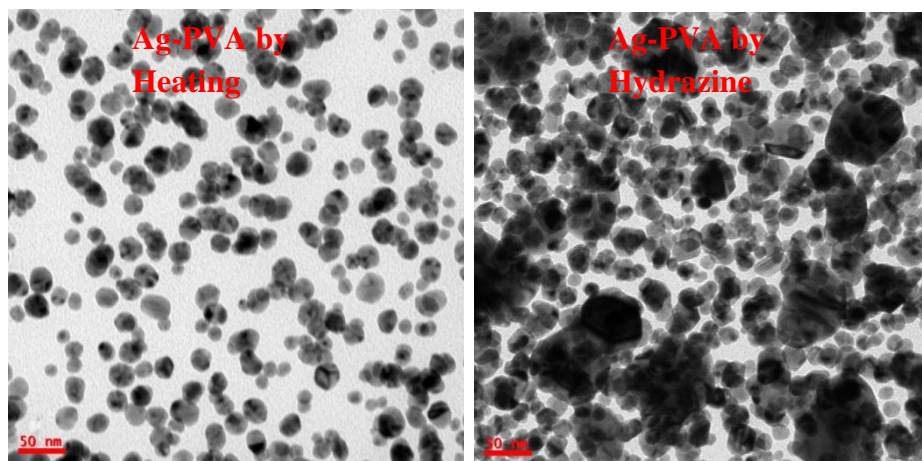


**Figure S7.** Extinction spectra of Ag-PVA fabricated with weight ratio ( $\text{Ag/PVA}$ ) = 1.0, by thermal treatment and exposing to hydrazine hydrate vapors at room temperature ( $\sim 28^\circ\text{C}$ ).



### TEM Images of the Ag-PVA Thin Films

**Figure S8.** TEM images (scale = 50 nm) of Ag-PVA fabricated with weight ratio (Ag/PVA) = 1.0, by thermal treatment and exposure to hydrazine hydrate vapors at room temperature ( $\sim 28^{\circ}\text{C}$ ).





## Electron Diffraction of the Cu-PVA, Cu-Ag-PVA and Ag-PVA Thin Films

### CuO-PVA and Cu-PVA thin films

**Table S4.** Indexing of the electron diffraction patterns recorded for the CuO-PVA and Cu-PVA thin films (Fig. 3c and 4c of the main text), based on the monoclinic structure of CuO and fcc structure of Cu.

ED pattern in	d (Å)	h k l
<b>Fig. 3c</b>	2.76	1 1 0 (CuO )
	2.50	$\bar{1}$ 1 1 (CuO)
	1.48	$\bar{1}$ 1 3 (CuO)
<b>Fig. 4c</b>	2.10	1 1 1 (Cu)
	1.81	2 0 0 (Cu)
	1.28	2 2 0 (Cu)
	1.07	3 1 1 (Cu)

### Cu-Ag-PVA thin films

**Table S5.** Indexing of the electron diffraction pattern recorded for the Cu-Ag-PVA thin film (Fig. 6 of the main text), based on fcc structures of Cu and Ag.

d (Å)	h k l
2.34	1 1 1 (Ag)
2.10	1 1 1 (Cu)
2.04	2 0 0 (Ag)
1.82	2 0 0 (Cu)
1.43	2 2 0 (Ag)
1.23	2 2 0 (Cu)
	3 1 1 (Ag)
1.04	2 2 2 (Cu)
	4 0 0 (Ag)

CuO: JCPDS file no: 89-2531

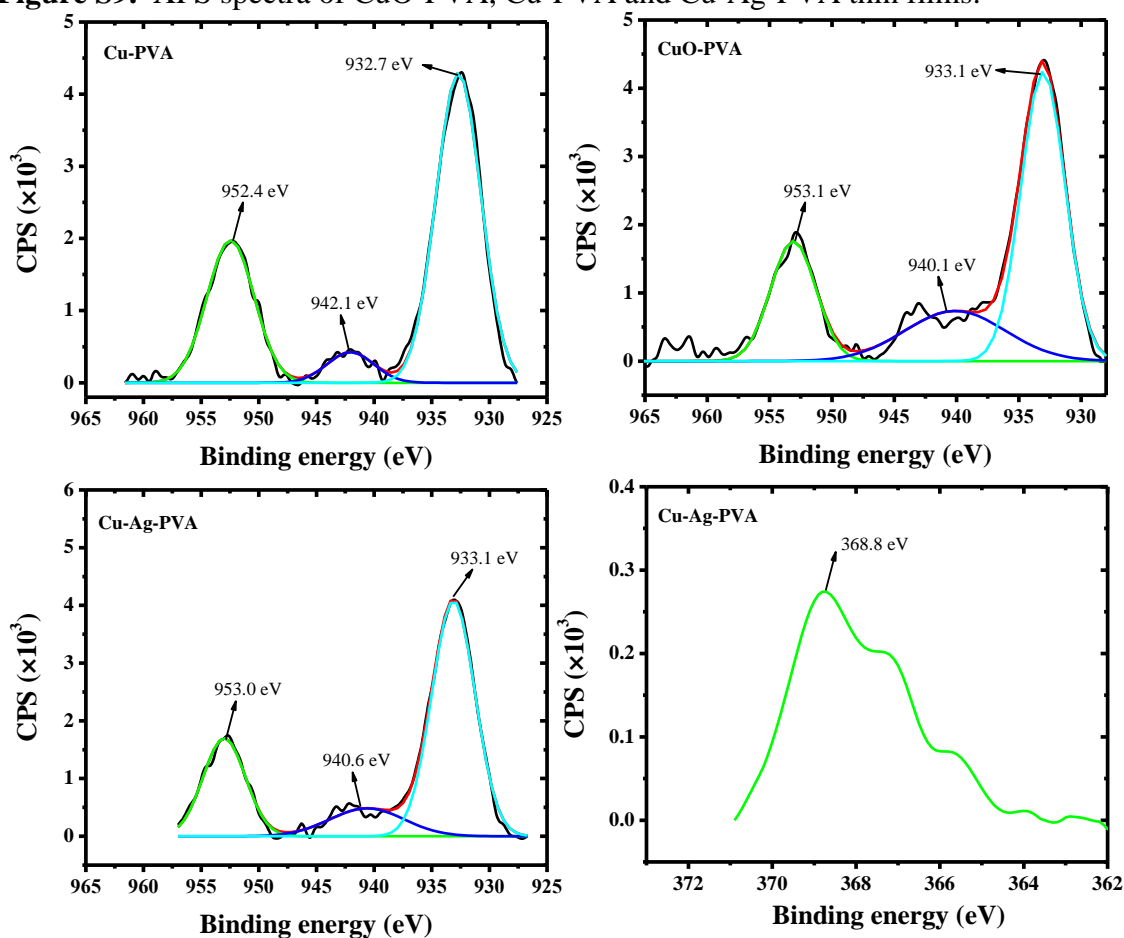
Cu: JCPDS file no: 01-1242

Ag: JCPDS file no: 01-1164

## X-ray Photoelectron Spectra

XPS of CuO-PVA, Cu-PVA and Cu-Ag-PVA (prepared with  $c = 12$  mM) thin films were recorded on a VG Microtech, model ESCA 3000 instrument equipped with ion gun (EX-05) for cleaning the surface; the binding energy resolution was 0.1 eV. Un-monochromatized Al  $K_{\alpha}$  radiation (photon energy = 1486.6 eV) was used where the electron take off angle (angle between electron emission direction and surface plane) was  $60^{\circ}$ . The core level binding energies were fixed with the carbon binding energy of 284.8 eV. Baseline corrected spectra with peak deconvolution are shown below.

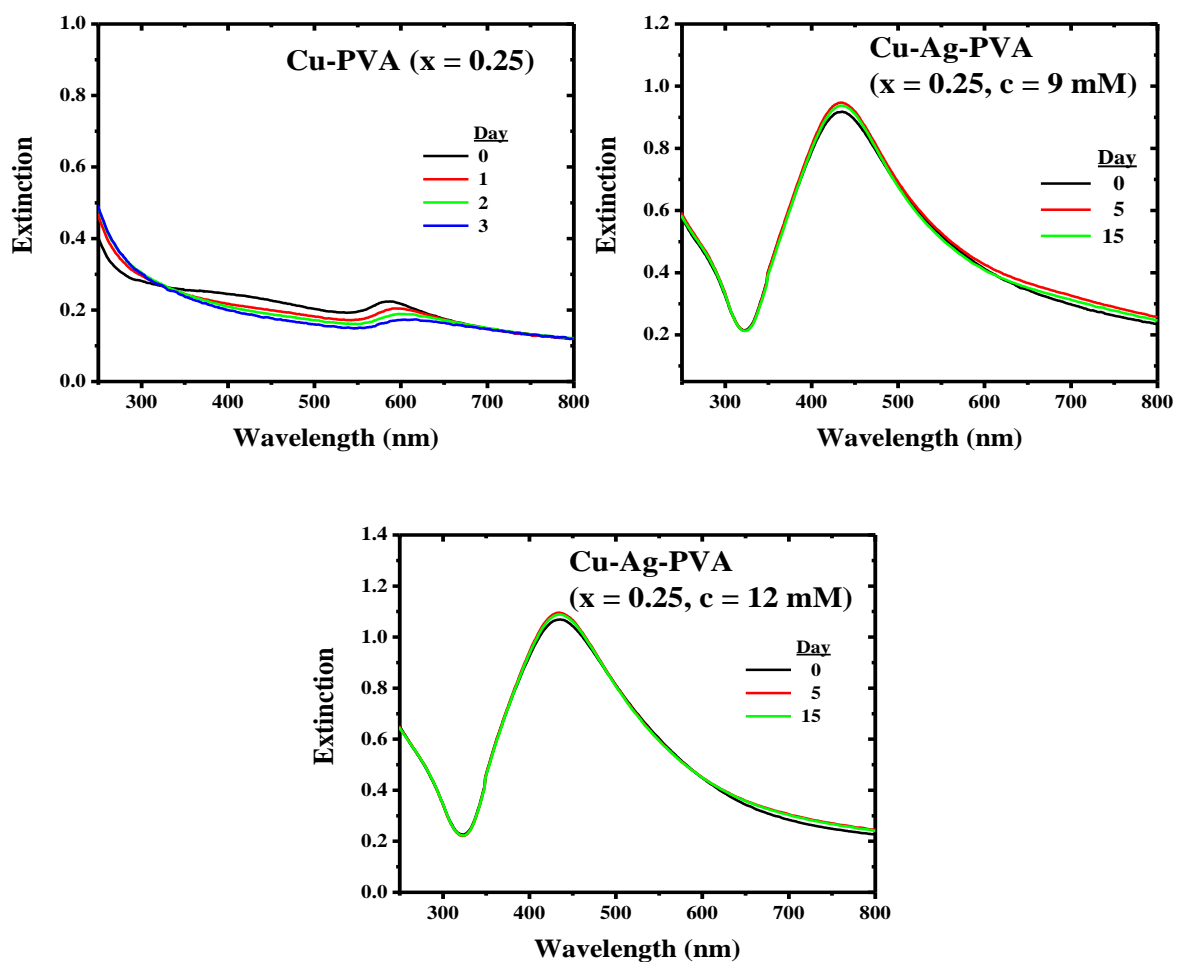
**Figure S9.** XPS spectra of CuO-PVA, Cu-PVA and Cu-Ag-PVA thin films.



**Cu-PVA** film shows  $2p_{3/2}$  and  $2p_{1/2}$  peaks of Cu at 932.7 and 952.4 eV; the satellite with peak at  $\sim 942.1$  eV appears to be due to partial oxidation of the Cu in the sample (Ref. 10 of main text). **CuO-PVA** film shows broadened  $2p_{3/2}$  and  $2p_{1/2}$  peaks with maxima at 933.1 and 953.1 eV and the satellite with peak at  $\sim 940.1$  eV; the broader peak is associated with the formation of Cu(II). **Cu-Ag-PVA** film shows the Cu  $2p_{3/2}$  and  $2p_{1/2}$  peaks at 933.1 and 953.0 eV and a weak satellite peak at  $\sim 940.6$  eV; peak due to Ag  $3d_{5/2}$  is observed at 368.8 eV. The shift in energies observed for the peaks with respect to Cu(0) and Ag(0) possibly arise due to the presence of each other.

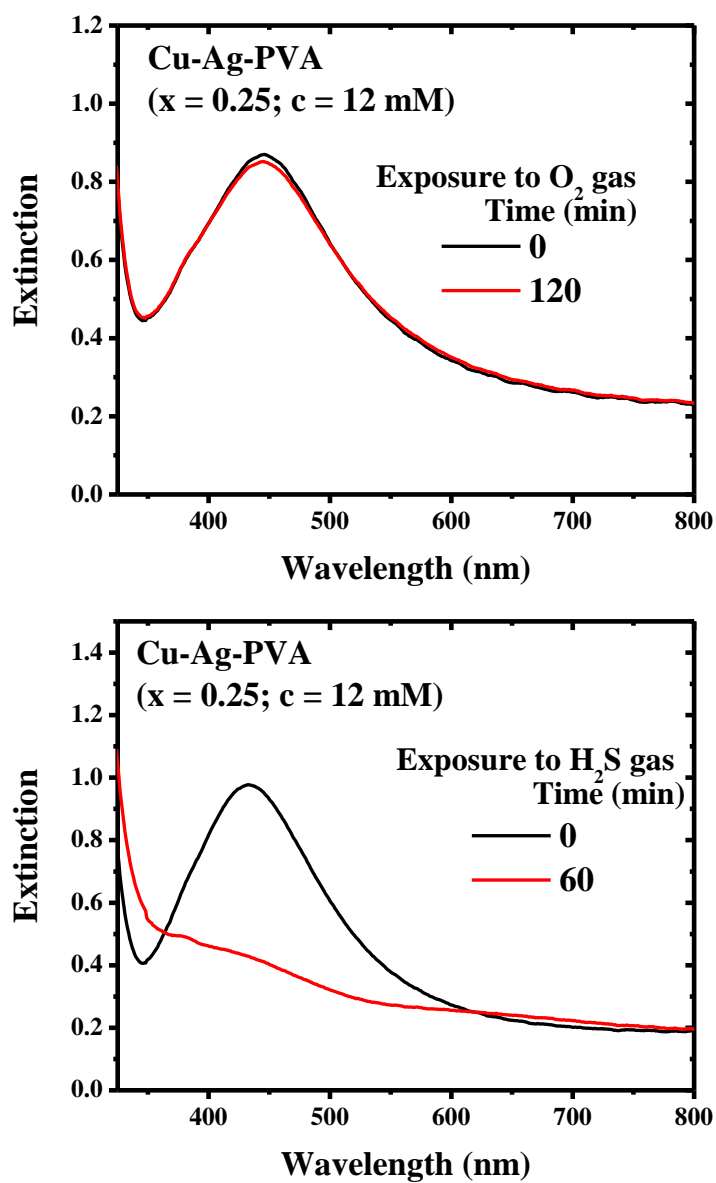
### Stability of the Cu-PVA and Cu-Ag-PVA Thin Films

**Figure S10.** Extinction spectra of Cu-PVA and Cu-Ag-PVA films recorded over different time intervals.



The spectra indicate clearly the improved stability of the Cu-Ag-PVA thin film, compared to the Cu-PVA thin film.

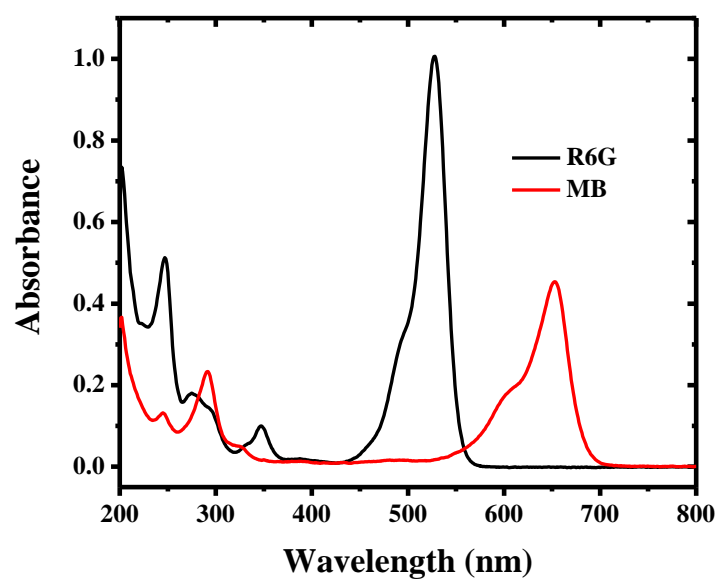
**Figure S11.** Extinction spectra of Cu-Ag-PVA thin film exposed to O<sub>2</sub> and H<sub>2</sub>S gases.



The spectra indicate clearly, that the Cu-Ag-PVA thin film is stable upon exposure to O<sub>2</sub> gas, whereas it is unstable under H<sub>2</sub>S gas.

### Absorption Spectra of R6G and MB

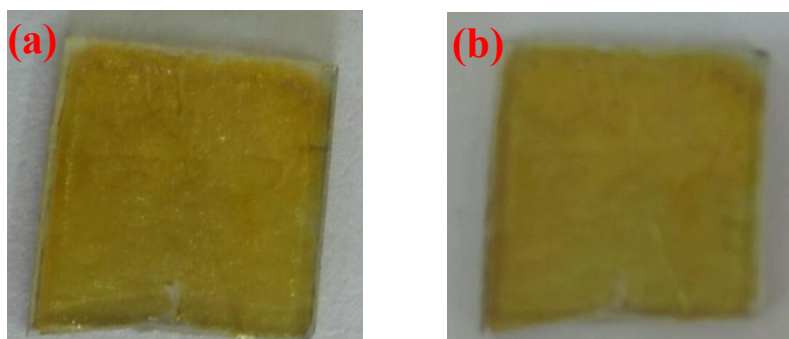
**Figure S12.** Absorption spectra of R6G and MB solutions used in the SERS experiments.



### Absorption of Analyte on Cu-Ag-PVA Thin Films

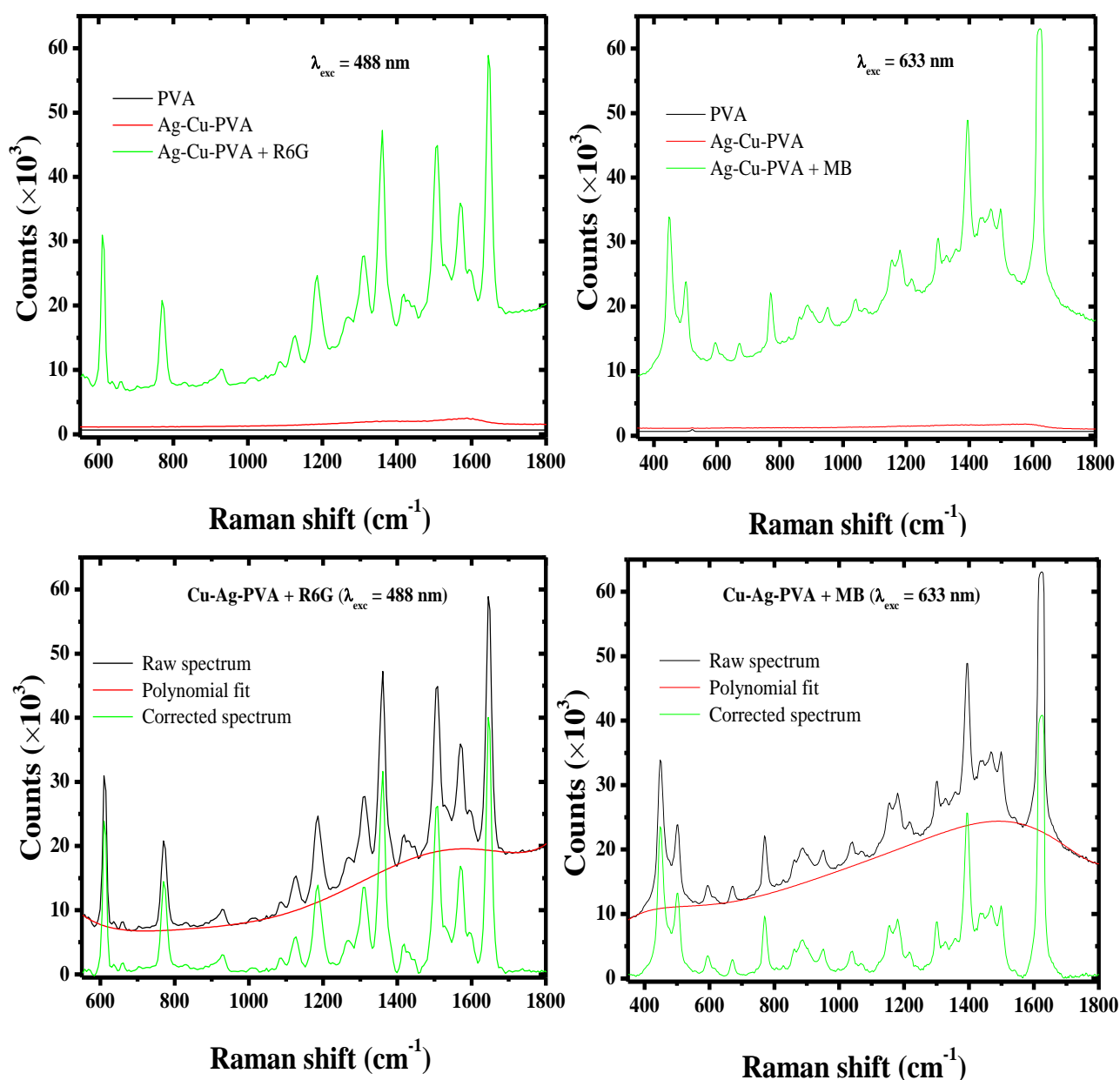
Uniform absorption of the analyte on the Cu-Ag-PVA thin films was confirmed by recording the Raman spectrum at different points on the thin film. Photographs of the film without and with R6G spread and absorbed on it, are shown below; appearance of the film changes only very slightly, as the concentration of the analyte is extremely low.

**Figure S13.** Photographs of Cu-Ag-PVA thin film ( $x = 0.25$ ;  $c = 6$  mM) on a glass substrate (a) without and (b) with R6G solution ( $\sim 16$   $\mu$ M) absorbed.



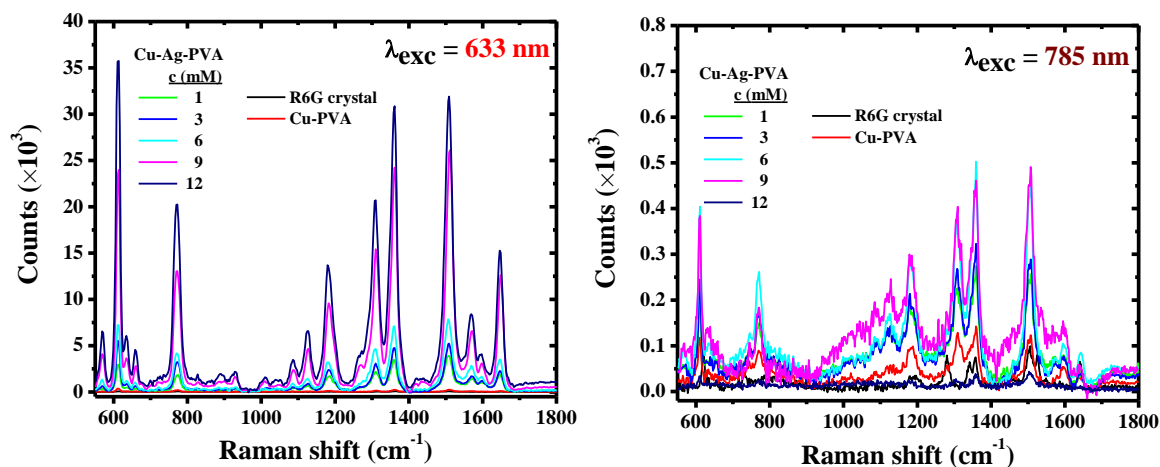
### Raman Spectra of PVA, Cu-Ag-PVA and Cu-Ag-PVA with R6G and MB

**Figure S14.** Raman spectra of PVA and Cu-Ag-PVA (without and with R6G (8.6  $\mu\text{M}$ ) and MB (6.3  $\mu\text{M}$ )) thin films, recorded using 488 and 633 nm laser excitation. The raw and corrected (for background due to fluorescence) spectra of Cu-Ag-PVA with R6G and MB are also shown.



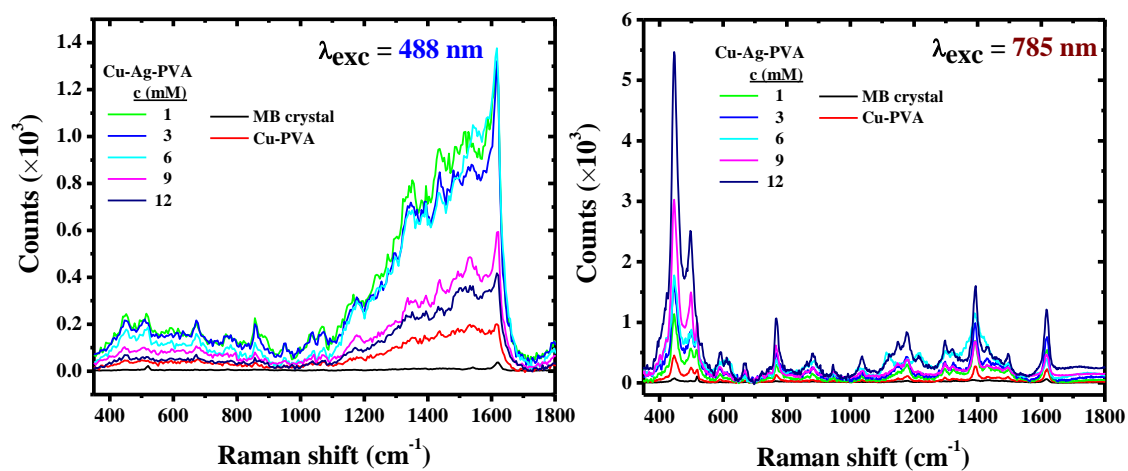
### Raman Spectra of R6G

**Figure S15.** Raman spectra of R6G solution (8.6  $\mu\text{M}$ ) on Cu-PVA ( $x = 0.25$ ) and Cu-Ag-PVA thin films fabricated by treatment of the Cu-PVA with different concentrations ( $c$ ) of  $\text{AgNO}_3$ , using 633 and 785 nm lasers as excitation.



### Raman spectra of MB

**Figure S16.** Raman spectra of MB solution (6.3  $\mu\text{M}$ , 20  $\mu\text{L}$ ) on Cu-PVA ( $x = 0.25$ ) and Cu-Ag-PVA thin films fabricated by treatment of the Cu-PVA with different concentrations ( $c$ ) of  $\text{AgNO}_3$ , using 488 and 785 nm lasers as excitation.





### Calculation of SERS Enhancement Factor

Laser spot diameter,  $W_o = \frac{1.22\lambda}{NA}$

Focal depth:  $Z_o = \left(\frac{2\pi}{\lambda}\right) W_o^2$

Focal volume:  $\tau = \left(\frac{\pi}{2}\right)^{1.5} W_o^2 Z_o$

$N_{\text{bulk}} = ((\text{Focal volume} * \text{Density}) / (\text{Molecular weight})) * N_A$

$N_{\text{SERS}} = (\text{Laser spot area} / \text{Substrate area}) * (N_A * \text{Volume} * \text{Concentration})$

$$\frac{N_{\text{bulk}}}{N_{\text{SERS}}} = \frac{\left(\frac{\pi}{2}\right)^{1.5} W_o^2 \left(\frac{2\pi}{\lambda}\right) W_o^2 \frac{\rho}{M} N_A}{\frac{\pi}{4} W_o^2 \frac{N_A VC}{A}} = \left(\frac{\pi}{2}\right)^{1.5} \left(\frac{8}{\lambda}\right) W_o^2 \frac{\rho}{M} \frac{A}{VC} = \frac{(2\pi)^{1.5}}{\lambda} W_o^2 A \frac{\rho}{w}$$

$$\frac{N_{\text{bulk}}}{N_{\text{SERS}}} = \frac{(2\pi)^{1.5}}{\lambda} \left(\frac{1.22\lambda}{NA}\right)^2 A \frac{\rho}{w} = 100 \times (2\pi)^{1.5} \times (1.22)^2 \frac{\lambda}{NA^2} \times A \times \frac{\rho}{w} = \frac{2344 \lambda}{NA^2} \times A \times \frac{\rho}{w}$$

$\lambda$  = Wavelength of the laser light (nm)

$NA$  = Numerical Aperture = 0.4

$A$  = Area of the film (cm<sup>2</sup>) = 3

$\rho$  = Density of the analyte crystal (g cm<sup>-3</sup>)

$\rho_{\text{R6G}} = 1.28$

$\rho_{\text{MB}} = 0.98$

$w$  = Weight of the analyte present in the solution spread on the film (ng)

$w_{\text{R6G}} = 82.39$

$w_{\text{MB}} = 40.3$

SERS enhancement factor =  $(N_{\text{BULK}} / N_{\text{SERS}}) * (I_{\text{SERS}} / I_{\text{BULK}})$

**Table S6.** Values of  $(N_{\text{BULK}} / N_{\text{SERS}})$  and  $I_{\text{BULK}}$  for R6G and MB used in the SERS experiments with different laser excitations.

$\lambda_{\text{exc}}$ (nm)	$N_{\text{BULK}} / N_{\text{SERS}} (\times 10^5)$		R6G		MB	
	R6G	MB	Peak (cm <sup>-1</sup> )	$I_{\text{BULK}}$	Peak (cm <sup>-1</sup> )	$I_{\text{BULK}}$
488	3.33	5.22	1645	58.72	1620	37.09
633	4.32	6.77	1509	86.30	1620	78.95
785	5.36	8.39	1506	99.00	445	74.59

**Table S7.** SERS enhancement factor (EF) for R6G on Cu-Ag-PVA thin film substrates fabricated by spreading different concentrations (c) of AgNO<sub>3</sub> on Cu-PVA (x = 0.25) thin films (a microcrystal of R6G is used as reference); data for Ag-PVA (with Ag/PVA weight ratio = 1.0, formed by heating as well as hydrazine treatment) substrate are also shown in the case of  $\lambda_{\text{exc}} = 488 \text{ nm}$ .

**(a)  $\lambda_{\text{exc}} : 488 \text{ nm}$**

Substrate		$I_{1645}$	$I_{\text{SERS}}/I_{\text{BULK}}$	EF ( $\times 10^8$ )
Cu-PVA		1137	19	0.06
Cu-Ag-PVA [c (mM)]	1	7180	122	0.41
	3	13643	232	0.77
	6	25314	431	1.44
	9	31169	531	1.77
	12	40063	682	2.27
Ag-PVA	Heating	8381	143	0.48
	Hydrazine	15140	258	0.86

[I = intensity of the aromatic C-C stretch vibration : microcrystal at  $1645 \text{ cm}^{-1}$  (I = 58.72)]

**(b)  $\lambda_{\text{exc}} : 633 \text{ nm}$**

Substrate		$I_{1509}$	$I_{\text{SERS}}/I_{\text{BULK}}$	EF ( $\times 10^8$ )
Cu-PVA		258	3	0.01
Cu-Ag-PVA [c (mM)]	1	3911	45	0.19
	3	5219	60	0.26
	6	7635	88	0.38
	9	26110	303	1.31
	12	31904	370	1.60

[I = intensity of the aromatic C-C stretch vibration : microcrystal at  $1509 \text{ cm}^{-1}$  (I = 86.30)]

**(c)  $\lambda_{\text{exc}} : 785 \text{ nm}$**

Substrate		$I_{1507}$	$I_{\text{SERS}}/I_{\text{BULK}}$	EF ( $\times 10^8$ )
Cu-PVA		123	1	0.01
Cu-Ag-PVA [c (mM)]	1	256	3	0.02
	3	288	3	0.02
	6	451	5	0.03
	9	491	5	0.03
	12	40	0.4	0.002

[I = intensity of the aromatic C-C stretch vibration : microcrystal at  $1506 \text{ cm}^{-1}$  (I = 99.00)]

**Table S8.** SERS enhancement factor (EF) for MB on Cu-Ag-PVA thin film substrates fabricated by spreading different concentrations (c) of AgNO<sub>3</sub> on Cu-PVA (x = 0.25) thin films (a microcrystal of MB is used as reference); data for Ag-PVA (with Ag/PVA weight ratio = 1.0, formed by heating as well as hydrazine treatment) substrate are also shown in the case of  $\lambda_{\text{exc}} = 633 \text{ nm}$ .

(a)  $\lambda_{\text{exc}} : 488 \text{ nm}$

Substrate		$I_{1620}$	$I_{\text{SERS}}/I_{\text{BULK}}$	EF ( $\times 10^8$ )
Cu-PVA		200	5	0.03
Cu-Ag-PVA [c (mM)]	1	1295	35	0.18
	3	1192	32	0.17
	6	1376	37	0.19
	9	593	16	0.08
	12	417	11	0.06

[I = intensity of the aromatic C-C stretch vibration : microcrystal at  $1620 \text{ cm}^{-1}$  (I = 37.09)]

(b)  $\lambda_{\text{exc}} : 633 \text{ nm}$

Substrate		$I_{1620}$	$I_{\text{SERS}}/I_{\text{BULK}}$	EF ( $\times 10^8$ )
Cu-PVA		611	8	0.05
Cu-Ag-PVA [c (mM)]	1	15933	202	1.37
	3	24310	308	2.09
	6	27594	350	2.37
	9	35464	449	3.04
	12	40687	515	3.49
Ag-PVA	Heating	977	12	0.08
	Hydrazine	2637	33	0.22

[I = intensity of the aromatic C-C stretch vibration : microcrystal at  $1620 \text{ cm}^{-1}$  (I = 78.95)]

(c)  $\lambda_{\text{exc}} : 785 \text{ nm}$

Substrate		$I_{445}$	$I_{\text{SERS}}/I_{\text{BULK}}$	EF ( $\times 10^8$ )
Cu-PVA		453	6	0.05
Cu-Ag-PVA [c (mM)]	1	1136	15	0.13
	3	1640	22	0.18
	6	1777	24	0.20
	9	3026	41	0.34
	12	5467	73	0.61

[I = intensity of the C-N-C deformation vibration : microcrystal at  $445 \text{ cm}^{-1}$  (I = 74.59)]

### Comparison of Enhancement Factors

**Table S9.** Comparison of the SERS EF of Cu-Ag based substrates reported earlier for different analytes using different excitation wavelengths with the present observations.

Ref. No	$\lambda_{\text{exc}}$ (nm)	Analyte	EF ( $\times 10^6$ )
4	514	R6G	*
11	514	R6G	1.1
12	785	Fluoranthene	0.21
13	633	R6G	*
14	780	Perchlorate	*
15	514	R6G	1.15
16	514	MBO	0.001
17	532	R6G	*
18	633	CV	*
19	514	R6G	1.0
20	532	R6G	2.5
21	633	4-ABT	1.4
22	514	CV	240
23	532	R6G	*
25	532	R6G	*
26	785	4-MBA	0.37
27	514	R6G	10.0
Present	488	R6G	227
	633	MB	349

\*Absolute value of EF is not reported

R6G : Rhodamine 6G

MBO : 2-mercaptobenzoxazole

CV : Crystal violet

MB : Methylene blue

4-ABT : 4-aminobenzenethiol

4-MBA : 4-mercaptobenzoic acid

### Limit of Detection

Standard deviation was estimated using Raman spectra recorded at 5 different positions on a substrate. The limit of detection was estimated as follows.

#### **R6G on Cu-Ag-PVA (c = 12 mM) [Fig. 10c (main text)]**

Least square fit line:  $\text{Counts } (\times 10^3) = 230.6 + 4771.5 \times [\text{R6G}]$

Slope of the least square fit line =  $4771.5 \mu\text{M}^{-1}$

Limit of detection (LOD) =  $(3 \times 52) / 4771.5 = 0.033 \mu\text{M}$

Volume of solution used =  $20 \mu\text{L}$

LOD in terms of number of mols =  $20 \mu\text{L} \times 0.033 \mu\text{M} = \mathbf{0.66 \text{ pmol}}$

#### **MB on Cu-Ag-PVA (c = 12 mM) [Fig. 10d (main text)]**

Least square fit line:  $\text{Counts } (\times 10^3) = 185.4 + 5943.6 \times [\text{MB}]$

Slope of the least square fit line =  $5943.6 \mu\text{M}^{-1}$

Limit of detection (LOD) =  $(3 \times 31) / 5943.6 = 0.016 \mu\text{M}$

Volume of solution used =  $20 \mu\text{L}$

LOD in terms of number of mols =  $20 \mu\text{L} \times 0.016 \mu\text{M} = \mathbf{0.32 \text{ pmol}}$